FOURIER IMAGE METHODS FOR EVOLUTION EQUATIONS OF DEEP-WATER WAVES

JAN JANKOWSKI[1] AND HENRYK LESZCZYŃSKI[2]

[1] *Polish Register of Shipping*
Gen. J. Hallera 126, 80-416 Gdańsk, Poland

[2] *Institute of Mathematics, University of Gdańsk*
Wita Stwosza 57, 80-308 Gdańsk, Poland

(received: 10 April 2019; revised: 15 May 2019;
accepted: 21 June 2019; published online: 10 July 2019)

Abstract: The velocity potential of the fluid satisfies the Laplace equation with nonlocal boundary conditions on a free surface. This differential problem is transformed to an evolution equation in Fourier variables. The Fourier transform images of boundary functions are approximated by Picard's iterations and the method of lines on meshes related to roots of Hermite polynomials. Due to convolutions of sine and cosine functions the integral terms of Picard's iterations reveal unexpected instabilities for wave numbers in a neighborhood of zero.

Keywords: Wave evolution, Laplace equation, Fourier transform, method of lines, Gauss-Hermite quadrature

DOI: https://doi.org/10.17466/tq2019/23.3/a

1. Introduction

We consider the following problem describing the velocity field V in terms of its potential $\Phi=\Phi(t,r,z)$, $r=(x_1,x_2)$, in the ocean with a free surface $\eta=\eta(t,r)$ varying in time

$$\begin{cases} \Delta\Phi+\frac{\partial^2\Phi}{\partial z^2}=0 & \text{for} \quad z<\eta(t,r) \\ \frac{\partial\eta}{\partial t}=\frac{\partial\Phi}{\partial n}\sqrt{1+|\nabla\eta|^2}=\frac{\partial\Phi}{\partial z}-\nabla\Phi\cdot\nabla\eta & \text{for} \quad z=\eta(t,r) \\ \frac{\partial\Psi}{\partial t}+g\eta=-\frac{1}{2}|\nabla\Phi|^2+\frac{1}{2}\left(\frac{\partial\Phi}{\partial z}\right)^2-\frac{\partial\Phi}{\partial z}(\nabla\Phi\cdot\nabla\eta) & \text{for} \quad z=\eta(t,r) \\ \lim\limits_{z\to-\infty}\Phi=0 \end{cases} \tag{1}$$

where $\Phi=\Phi(t,r,z)$ is the velocity potential in the sea domain

$$\left\{(r,z)\in\mathbf{R}^3\colon\ -\infty<z<\eta(t,r)\right\} \tag{2}$$

$\nabla = \left(\frac{\partial}{\partial x_1}, \frac{\partial}{\partial x_2}\right)$, $\Delta = \frac{\partial^2}{\partial x_1^2} + \frac{\partial^2}{\partial x_2^2}$ and $\Psi(t,r) = \Phi(t,r,\eta(t,r))$. The system of Equations (1) is valid for the incompressible, non-viscous, non-rotational fluid and conserves the total energy of the fluid (see [1, 2])

$$E := \frac{1}{2} g \int \eta^2 dr + \frac{1}{2} \int\limits_{z \le \eta(r)} \left[|\nabla \Phi|^2 + \left(\frac{\partial \Phi}{\partial z} \right)^2 \right] dz dr \tag{3}$$

The equations in (1), which constitute a boundary-value problem on the sea free surface, were derived by Zakharov from the Hamilton equations

$$\frac{\partial \eta}{\partial t} = \frac{\delta E}{\delta \Psi}, \quad \frac{\partial \Psi}{\partial t} = -\frac{\delta E}{\delta \eta} \tag{4}$$

applied to the variation of energy. η and Ψ are canonical variables and the energy of the water is the Hamiltonian. Various mathematical models describing the generation of waves by wind have been developed during the last century. The latest research on wave processes and modeling is described in the books [3] and [4]. In general, the structure of these books comprises the formulation of a nonlinear equation describing the fluid flow generated by the surface wave motion, the total energy of the fluid in motion, the sea surface winds and the physical description of wave evolution, including the wave-wave interaction and the non-linear energy transfer. An important part of these books is devoted to the numerical modeling of the wave evolution and its applications to the wave hindcasting and forecasting.

The principles of wave prediction have been already known since the beginning of the 1960s. It was necessary to introduce certain simplifications in the energy balance equation at that time, as reported and explained in [5], because:

- the role of wave-wave interactions in the wave evolution had not been recognized yet,
- the limited computer power precluded the use of any nonlinear transfer in the energy balance equation.

The importance of the nonlinear transfer and the wind input became more evident after measurements of the wind input to waves and growth of the caused by the wind input, *e.g.* [6], [7].

Zakharov [1] studied the stability of nonlinear waves on the surface of infinitely deep water. He described this phenomenon under the assumption that the flow was irrotational and the fluid was incompressible (potential flow), which resulted in the Laplace equation in the fluid and nonlinear equations on the free surface (1). The solution of the boundary-value problem (1) is sought in the series form in powers of η. The Fourier transform with respect to the space variable $r = (x_1, x_2)$ is applied to obtain the series in a more convenient form. Such approach enabled Zakharov to determine a functional series expansion for Φ in the image of this transform up to the second-order terms of η. In further considerations simplifying assumptions were introduced to create heuristic models of the flow rather than solving this problem in a strict mathematical manner.

Since the differential problem considered in Zakharov's papers is extremely difficult to solve analytically in a closed form and any detailed presentation of the theory in a short article is hard to convey (*cf.* [1]), we attempt to solve problem (1) in the image of the Fourier transform. The Fourier transform of $f=f(r)$ is denoted as $f=f(k)$ instead of $\widehat{f}(k)$. We do not study the unknown functions $\Phi=\Phi(t,r,z)$, $\Psi=\Psi(t,r)$, $\eta=\eta(t,r)$ in the sequel, but we deal with their Fourier transforms $\Psi=\Psi(t,k)$, $\eta=\eta(t,k)$.

Differential equations for the boundary potential flow and the free surface in the image of the Fourier transform with the use of a kind of a power series with respect to η are formulated in Section 2. Picard's iterations for solving these equations, truncated to the second order nonlinear terms, are presented there. The integral terms contain convolutions of sine and cosine functions. These convolutions show unexpected instabilities for wave numbers in a neighborhood of zero. A discretization of the differential-functional equations by the method of lines (MOL) with a mesh generated by zeros of Hermite's polynomials is also presented. The Gauss-Hermite quadrature is used to approximate the integrals over $\mathbb{R}^2$. Discussions and conclusions in Section 3 summarize the main results of the paper. In particular, we compare Picard's iterations and the method of lines. The main conclusion of the paper is that the solution of the truncated differential problem including second order nonlinear terms reveals new possibilities of wave instabilities, in contradiction to the literature where second order terms are neglected for some reasons, whereas third order terms, creating Boltzmann-type interactions between wave numbers, are considered in [8].

Taking into account the above-mentioned ways of solving problem (1), it seems indispensable to apply a strictly mathematical approach to solve this problem in order to confirm the existing knowledge or obtain new information. This paper presents the first stage of this approach.

2. Picard's iterations and the method of lines

The functions η,Ψ (the free surface and the boundary potential in the Fourier image) satisfy the nonlocal differential equations:

$$\begin{aligned}\frac{\partial\eta(t,k)}{\partial t}=&|k|C(t,k)+\sum_{j=1}^{\infty}\frac{1}{j!(2\pi)^j}\int C(t,\bar{k})\eta(t,k_1)...\eta(k_j)\\&\times|\bar{k}|^{j-1}\left(|\bar{k}|^2+j(k_j\cdot\bar{k})\right)\delta\left(k-\bar{k}-k_1-...-k_j\right)dk_1...dk_jd\bar{k}\end{aligned}\tag{5}$$

$$\begin{aligned}\frac{\partial\Psi(t,k)}{\partial t}=&-g\eta(t,k)+\frac{1}{4\pi}\sum_{j=0}^{\infty}\frac{1}{j!(2\pi)^j}\int C(t,\bar{k})C(t,\tilde{k})\eta(t,k_1)...\eta(k_j)\\&\times\left(|\bar{k}|+|\tilde{k}|\right)^{j-1}\left[\left(\bar{k}\cdot\tilde{k}+|\bar{k}||\tilde{k}|\right)\left(|\bar{k}|+|\tilde{k}|\right)+2j|\tilde{k}|\left(k_j\cdot\bar{k}\right)\right]\\&\times\delta\left(k-\bar{k}-\tilde{k}-k_1-...-k_j\right)dk_1...dk_jd\bar{k}d\tilde{k}\end{aligned}\tag{6}$$

with an auxiliary function $C(t,k)$ dependent on $\eta=\eta(t,k)$, $\Psi=\Psi(t,k)$. These equations are based on the formal solution of the Laplace equation. The linearization

of the system of nonlinear PDEs (5)–(6), yields a linear ODE system with the parameter k

$$\frac{d}{dt}\begin{bmatrix}\eta\\ \Psi\end{bmatrix}=\begin{bmatrix}0 & |k|\\ -g & 0\end{bmatrix}\begin{bmatrix}\eta\\ \Psi\end{bmatrix} \tag{7}$$

Picard's iterations (η^i,Ψ^i) can be applied to the nonlinear integral equations (5) and (6), which start from (7). The right-hand side contains convolutions of sine and cosine functions with their multiplications.

We discretize the differential functional equation (5)–(6) by the method of lines (MOL) with a mesh generated by zeros of Hermite's polynomials. Let $\zeta_1,...,\zeta_N$ be all zeros of $H_N(\zeta)$. The Gauss-Hermite quadrature with coefficients $\mathbf{A}_1,...,\mathbf{A}_N$ is applied to approximate integrals over $\mathbf{R}^2$. We are looking for $\left(\eta^{(i)}(t),\Psi^{(i)}(t)\right)$, $i=(i_1,i_2)$, $i_1,i_2=1,...,N$ which approximate $(\eta(t,k),\Psi(t,k))$ at the points $k=k^{(i)}=(\zeta_{i_1},\zeta_{i_2})$.

$$\frac{d}{dt}\begin{bmatrix}\eta^{(i)}\\ \Psi^{(i)}\end{bmatrix}=\begin{bmatrix}0 & |k^{(i)}|\\ -g & 0\end{bmatrix}\begin{bmatrix}\eta^{(i)}\\ \Psi^{(i)}\end{bmatrix}+\frac{1}{2\pi}\sum_j \mathbf{A}_{j_1}\mathbf{A}_{j_2}e^{|k^{(j)}|^2} \tag{8}$$
$$\times\begin{bmatrix}\Psi^{(j)}I_N\eta(k^{(i)}-k^{(j)})\left(\bar{k}^{(i)}\cdot k^{(i)}-|k^{(j)}||k^{(i)}|\right)\\ \frac{1}{2}\Psi^{(j)}I_N\Psi(k^{(i)}-k^{(j)})\left(k^{(j)}\cdot(k^{(i)}-k^{(j)})+|k^{(j)}||k^{(i)}-k^{(j)}|\right)\end{bmatrix}$$

Equation (8) together with an initial condition $\eta^{(i)}(0)=\eta_0(k^{(i)})$, $\Psi^{(i)}(0)=\Psi_0(k^{(i)})$ is a complete definition of the method of lines. Our numerical experiments concerning approximations of (5)–(6) are performed with the initial functions $\eta_0(k)=0$, $\Psi_0(k)=\exp(-|k|^2)$. These functions clearly belong to the Schwartz space $\mathcal{S}(\mathbb{R}^2)$. They are symmetric, hence, the computer algorithms demand much less time.

The results of numerical computations are presented in several figures. The pair of Figures 1–2 show a comparison of numerical solutions of the differential problem by means of two methods: MOL and Picard's iteration, in points of the plane $k=k^{(i)}=(\zeta_{i_1},\zeta_{i_2})$ indicated on the graphs. For the graphical presentation of the results of numerical computations, the mesh nodes are selected at a relatively large distance from zero $k=(0,0)$, namely $|k|\approx 4$, where the values η and Ψ are very small. These nodes depend on the number of Hermite's polynomial zeros and they cannot be equal to each other on the meshes of 10×10, 20×20 and 50×50 nodes. Therefore, for the purpose of comparison the graphs are generated by computations in the nearest nodes. Each figure presents results obtained with the use of the Gauss-Hermite quadrature with 10, 20 and 50 zeros of Hermite's polynomials H_{10}, H_{20}, H_{50} to approximate integrals over $\mathbb{R}^2$. The figures show that:

- both methods produce numerical solutions $(\eta^{(i)},\Psi^{(i)})$ which agree with each other;
- the increase in the degree of Hermite's polynomials in the Gauss-Hermite quadrature increases the accuracy of the solution in the sense that $(\eta^{(i)},\Psi^{(i)})$

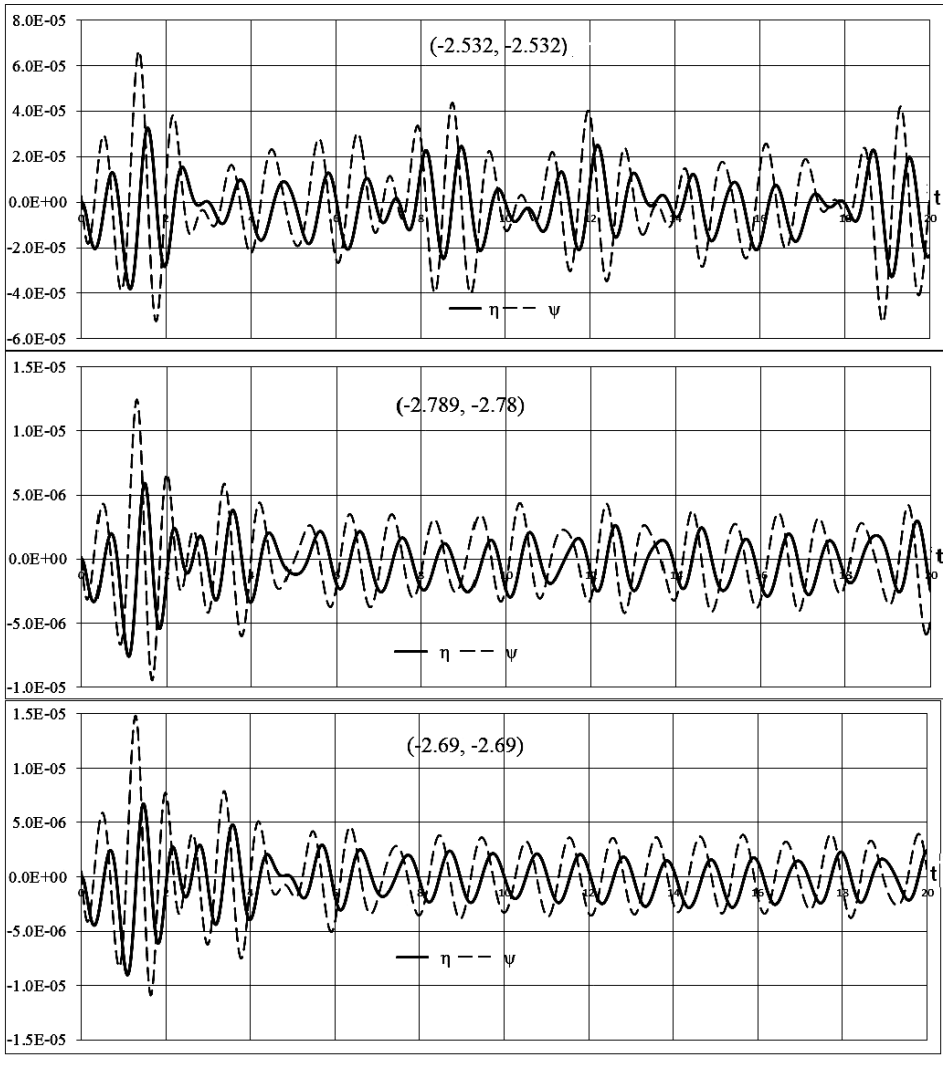

Figure 1. MOL with G-H quadratures: 10, 20, 50 zeros. Horizontal axes t stand for time, vertical axes denote values of η and Ψ

based on 20×20 and 50×50 mesh-point quadratures are almost the same (just the use of 20 zeros seems to be sufficient), while those based on the 10×10 mesh points differ from them.

The initial conditions prescribed cause that close to the origin $k^{(i)}=(0,0)$ the linear part of the solution $(\eta^{(i)},\Psi^{(i)})$ dominates over the nonlinear part, while in points distant from $k^{(i)}=(0,0)$ the nonlinear part prevails. Figure 3 presents the function $\Psi(t,k)$ for $k\in[-3,3]\times[-3,3]$, obtained by a spline interpolation of the numerical solution $\Psi=\Psi(t,k^{(i)})$ with $t=6.29[s]$. However, nodes of the mesh in which the differential problem is solved are rather sparse in the plane (ζ_1,ζ_2), so a question might be asked about possible oscillations between the nodes defined

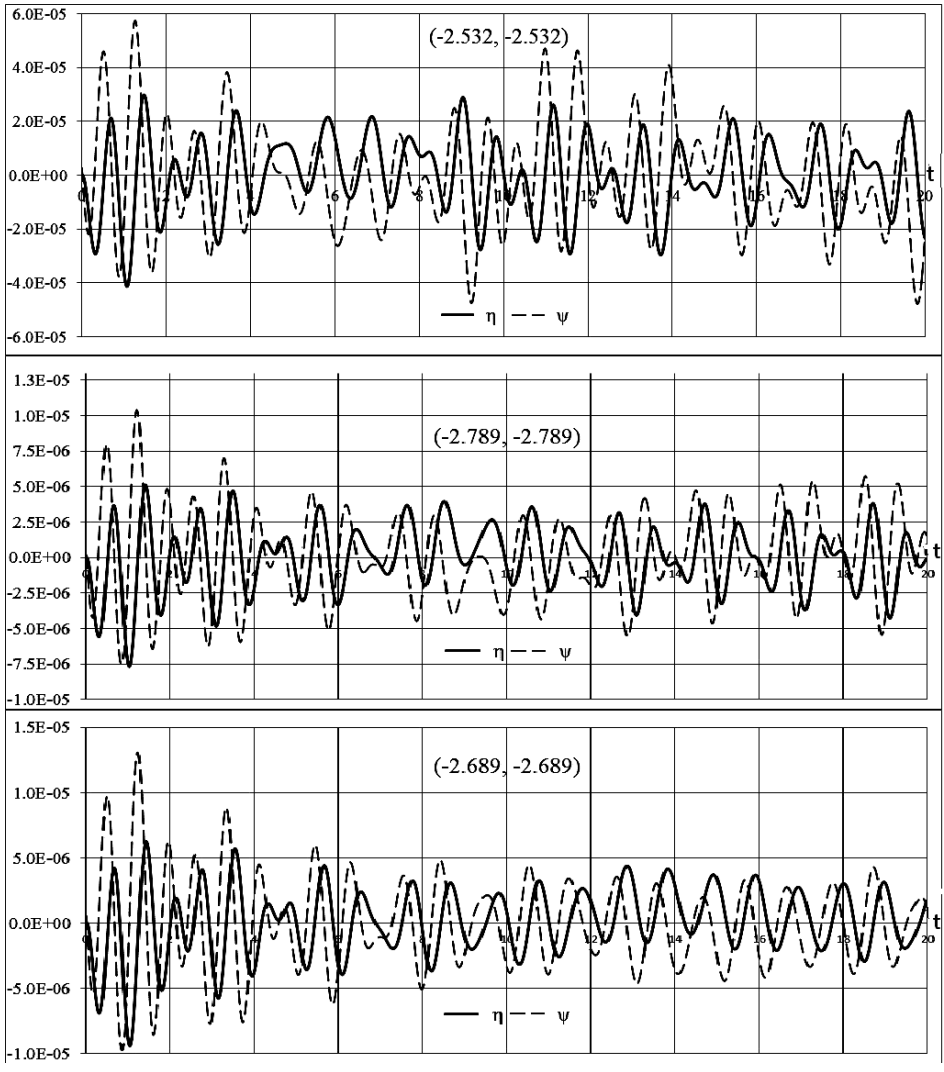

Figure 2. Picard's iterations with G-H quadratures: 10, 20, 50 zeros. Horizontal axes t stand for time, vertical axes denote values of η and Ψ

by zeros of Hermite's polynomials. The solution of the linear part of this problem on a dense regular mesh for $k_1 \in [-3,3]$, $k_2 = 0$ and for $t = 6.29[s]$ confirms this conjecture. Our numerical practice leads to a slightly pessimistic claim that the Gauss-Hermite quadrature is not the best one to approximate integrals over $\mathbb{R}^2$.

3. Discussions and conclusions

We summarize and conclude the results of our paper in several items.

(i) There are at least two sources of weak singularity near $k = 0$, $\bar{k} = 0$, $k - \bar{k} = 0$:

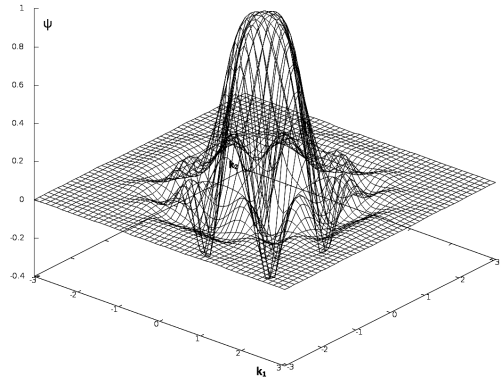

Figure 3. 3D illustration of $\Psi(t,k)$ for $t=6.29$ where $k=(k_1,k_2)$

- the fundamental matrix $E(t,k)$ of Equation (7) contains coefficients like $1/\sqrt{|k|}$;
- the convolutions of sine and cosine functions either have high oscillations or approach a straight line or another non-periodic curve.

(ii) Let us admit that Equation (7) is a vector-valued version of the single equation $\partial a/\partial t + i\omega a = 0$ where $a = a(t,k)$ is a kind of complexification of (η,Ψ), $\omega = \sqrt{g|k|}$. The literature is focused on instabilities generated by third-order terms like $a_1 a_2 a_3^*$, see [1], which is due to an aggregation of waves around manifolds

$$k_1 + k_2 - k_3 - k_4 = 0, \quad \sqrt{|k_1|} + \sqrt{|k_2|} - \sqrt{|k_3|} - \sqrt{|k_4|} = 0 \tag{9}$$

Our paper reveals certain possibilities to create instabilities by second-order terms. This is seen in convolutions of sine and cosine functions, which produce combinations of $\sqrt{|k|} \pm \sqrt{|\bar{k}|} \pm \sqrt{|k-\bar{k}|}$ in denominators. We show an example for $k=(1,0)$ in Figure 4. The resonance effect appears despite very regular initial functions η_0, Ψ_0, and is confirmed by both approximation methods: Picard's iterations and the method of lines. It produces difficulties in any implementation of numerical schemes. Gauss-Hermite quadratures have positive coefficients and good stability properties, however, an exact explanation why MOL and Picard's iteration is not influenced too much by odd effects in a neighborhood of $(0,0)$ is unknown. We performed MOL experiments with a regular mesh and the trapezoidal rule. All quantitative and qualitative effects are very similar to those presented in our paper. The time of computations is much longer.

(iii) The differential problem (1) should be solved in a subset of the Schwartz space $\mathcal{S}(\mathbb{R}^2)$ of smooth functions vanishing at infinity together with all derivatives, therefore, the initial data must belong to this space. In the literature this fact is taken for granted. Any attempt to prove rigorous estimates leads to hopeless integral inequalities.

(iv) In our further investigations, we plan to use two approaches:

- to apply at least two Picard iterations to solve problem (5)–(6) and obtain new information concerning unexpected properties of waves – Picard's iterations

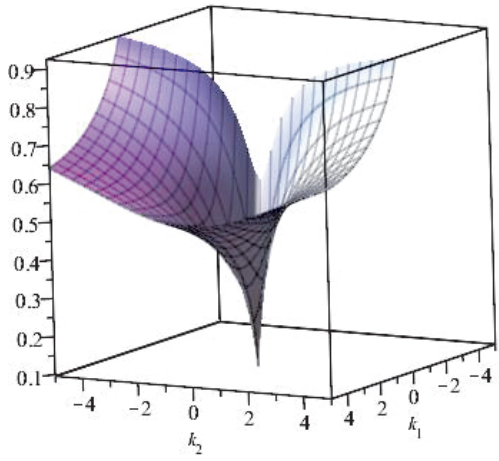

Figure 4. Singularity $\sqrt{|k|} \pm \sqrt{|\bar{k}|} \pm \sqrt{|k-\bar{k}|}$ for $k = (1,0)$

reveal singularities on manifolds in two- and four-dimensional spaces of wave numbers, which result from the assumption on the potential flow. Information about these singularities is essential for a proper solution of the boundary-value problem (1);

- to assume that the solution of problem (5)–(6) has the form of series of functions with separated variables (time t and Fourier variables k), where time-dependent functions will be unknown variables, enabling to solve the main problem in $\mathbb{R}^2$.

References

[1] Zakharov V E 1968 *Zhurnal Prikladnoi Mekhaniki i Tekhnicheskoi Fiziki* **9** (2) 190
[2] Stiassnie M and Shemer L 1984 *J. Fluid Mech.* 47
[3] Komen G J, Cavaleri L, Donelan M, Hasselmann K, Hasselmann S and Janssen P A E M 1994 *Dynamics and Modelling of Ocean Waves*, Cambridge University Press
[4] Lannes D 2013 *AMS.* **188**
[5] Part VII: ECMWF Wave Model, IFS Documentation – Cy40r1, Operational implementation 2013 [online:] `https://www.ecmwf.int/sites/default/files/IFS_CY40R1_Part7.pdf`
[6] Mitsuyasu H 1968 *On the growth of the spectrum of wind-generated waves. II*, *Rep. Res. Inst. Appl. Mech. (Kyushu Univ.)* **17** (59) 235
[7] Hasselmann K, Barnett T P, Bouws E, Carlson H, Cartwright D E, Enke K, Ewing J A, Gienapp H, Hasselmann D E, Kruseman P, Meerburg A, Müller P, Olbers D J, Richter K, Sell W and Walden H 1973 *Measurements of wind-wave growth and swell decay during the Joint North Sea Wave Project (JONSWAP)*, *Dtsch. Hydrogr. Z. Suppl. A* **8** (12)
[8] Hasselmann S, Hasselmann K 1985 *Journal of Physical Oceanography* **15** 1369